Assessing Movement Patterns using Bayesian State-Space Models on Lake Winnipeg Walleye

Munaweera I[a], Muthukumarana S[a], Gillis D M[a], Watkinson D A[b], Charles C[b], and Enders E C[b]

[a]University of Manitoba,

Winnipeg R3T 2N2.

[b]Fisheries and Oceans Canada,

501 University Cres.

Winnipeg MB R3T 2N6

Corresponding author: Inesh Munaweera

Address: 318 Machray Hall University of Manitoba, Winnipeg, MB R3T 2N2 Canada

Telephone: 12049513368

E-mail: ineshpma@myumanitoba.ca

Manuscript prepared for Canadian Journal of Fisheries and Aquatic Sciences

Abstract

Acoustic telemetry systems technology is useful for studying fish movement patterns and habitat use. However, the data generated from omnidirectional acoustic receivers are prone to large observation errors since the tagged animal can be anywhere in the detection range of the receiver. In this study, we used the Bayesian state-space modeling (SSM) approach and different smoothing methods including kernel smoothing and cross-validated local polynomial regression to reconstruct fish movement paths of Walleye (*Sander vitreus*) using data obtained from a telemetry receiver grid in Lake Winnipeg. Using SSM approach, we obtained more realistic movement paths, compared to the smoothing methods. In addition, we highlighted the advantages of the SSM approach to estimate undetected movement paths, over simple smoothing techniques, by comparing ecological metrics such as path length and tortuosity between different reconstruction approaches. Reconstructed paths could be useful in making effective fishery management decision on Lake Winnipeg in the future by providing information on how Walleye move and distribute in Lake Winnipeg over space and time.

Keywords: Acoustic Telemetry, Walleye, Bayesian Inference, Markov Chain Monte Carlo, State Space Models, Fish Movements.

Introduction

Fish can be highly mobile in the search for suitable foraging and spawning habitats (Cooke et al. 2016). Fish movement paths reveal habitat use, migration patterns, survival, and behavioural changes across years. Understanding how fish distribute and survive over space and time is important for sustainable resource management. For instance, by identifying critical habitats and movement patterns, a fishery manager can be informed of any potential risks that the fish in a population might experience from commercial fishing gear and other human activities. This will allow the manager to make effective fish management and conservation decisions (Brownscombe et al. 2019; Cooke et al. 2004, 2016).

Unlike most terrestrial animals, studying freshwater fish is not a simple task due to the complex nature of their habitats and the poor visibility in water (Cooke et al. 2016). However, modern tracking technologies such as acoustic telemetry allow for the collection of an enormous amount of data on animal movements over long distances without directly observing them in their natural habitats (Donaldson et al. 2014; Jonsen et al. 2003; Klimley et al. 1998).

Traditional acoustic telemetry studies frequently consist of an arrangement of receivers at geographical bottlenecks, which is suitable for a broader study of movements such as migration across the landscape or aquatic habitat Cooke et al. (2011). A linear arrangement of receivers does not help in understanding movements throughout a region. In this case, a systematically deployed two-dimensional array of receivers can be used (Kraus et al. 2018). However, the data collected by widely used omnidirectional acoustic receivers are subject

to large observation errors, especially when the distance between two adjacent receivers in the array is large (Alós et al. 2016). Hence, the detection of an acoustic tag only suggests proximity, but does not reveal the true location. Furthermore, the probability of a fish being detected by a receiver decreases as the fish moves away from the receiver, and the detection probability is also affected by environmental variables such as ice-cover, wind, and wave action (Klinard et al. 2019; Reubens et al. 2019). Two main approaches are available to estimate fish movement paths: (1) detection records can be smoothed to obtain the average fish locations for regular time bins, and (2) fish locations are estimated based on an underlying process model that describes fish behaviour.

Several different smoothing techniques have been applied to movement data. Simpfendorfer et al. (2002) used the weighted means algorithm to estimate the average fish locations. Hedger et al. (2008) suggested using the cross-validated local polynomial regression with Friedman's super smoother (Friedman 1984) to be the optimum interpolation method. Furthermore, Hedger et al. (2008) recommended kernel estimation with the Gaussian kernel to interpolate fish paths. Even though smoothing techniques provide an easily implemented and efficient way to reconstruct movement paths, simply smoothing the detection path mask the actual fish movement behaviour. This can lead to incorrect estimates of ecological metrics such as swimming speed and total distance traveled. These are important in quantifying individual fish movement for use in further analysis such as comparing behavioural patterns among individual fish (Seidel et al. 2018).

Bayesian state-space modelling (SSM) is a promising approach for modeling individual-level animal movement. In ecology, SSMs are widely used for studying animal movements

since they can account for both, process variation, which is the natural variation of the underlying movement process and the observational error, which is the difference between the observed position and the true position of the animal (Albertsen et al. 2015; Alós et al. 2016; Bolker 2008; Patterson et al. 2017, 2008). Also, within the SSM approach, it is possible to incorporate additional information such as prior knowledge and detection probabilities in the estimation. Pedersen and Weng (2013) developed an SSM for observation network data to estimate animal movement using the Ornstein-Uhlenbeck (OU) process. They used the OU process based SSM to estimate movement paths and home range of Humphead Wrasse (*Cheilinus undulatus*; a coral reef fish). Through simulations, they showed that the SSM outperformed the smoothing techniques suggested by Hedger et al. (2008) and Simpfendorfer et al. (2002). Alós et al. (2016) used a more sophisticated SSM with a mechanistic movement model that accounted for the fish's home range behaviour to reconstruct individual movement patterns of Pearly Razorfish (*Xyrichtys novacula*) within a short time period of 20 days using acoustic telemetry data. They performed a simulation study to assess the accuracy and the precision of their model and found that SSM models provide accurate and unbiased estimates for the movement parameters and locations.

The objective of this study was to develop a framework to effectively reconstruct individual fish movement paths to infer Walleye behaviour in Lake Winnipeg. As a part of the Lake Winnipeg Basin Fish Movement Project, 357 Walleye (*Sander vitreus*) were tagged and a grid of acoustic receivers was deployed in Lake Winnipeg and some of its major tributaries to detect the movements of tagged fish. From June 2017 to September 2018, the receivers recorded over 3.8 million detections. To achieve our objective, we used Bayesian SSMs and

three popular smoothing approaches (simple weighted average method, kernel smoothing with the Gaussian kernel, and cross-validated local polynomial regression approach) to reconstruct fish movement paths. Furthermore, we performed a simulation study to evaluate the performance of the different modeling approaches in estimating the movement paths.

Materials and methods

Study area

Lake Winnipeg, located in Manitoba, Canada, is the tenth largest lake in the world by surface area (24,514 km^2) and accounts for North America's second-largest freshwater fishery (Sheppard et al. 2015; Wassenaar and Rao 2012). It is a shallow lake that has two main basins (north basin and south basin), that are connected through the narrows (Fig. 1). The average depth of the north basin is 13.3 m and, the south basin is only 9 m deep on average (Brunskill et al. 1980; Stewardship et al. 2011). The lake typically has ice form around the middle of November in both basins, and ice melting usually at the end of April to mid-May in the south basin and mid-May to early June in the north basin. Despite its importance to commercial fisheries, little research has been conducted to understand how fish respond to the fishing pressure and changes in the physical environment (Johnston et al. 2012).

Study species

Walleye are large-bodied piscivorous fish that are commonly found in moderately productive lakes in North America (Hartman 2009). Adult Walleye typically reach maturity at lengths

ranging from 35–50 cm. Spawning occurs in early spring from mid-April to the end of May in Manitoba. Walleye is the most valuable species for commercial and recreational fisheries in Lake Winnipeg (Fisheries and Canada 2020; Stewart and Watkinson 2004; Thorstensen et al. 2020).

Experimental setup and procedure

For tagging, fish were captured by boat electrofishing. Only individuals with a body mass >1.2 kg were tagged ensuring that the transmitter was less than 2% of the mass of the fish. 'Vemco V16-4H' acoustic transmitters (16 mm diameter, 24 g, 6 $\frac{1}{2}$ years expected battery life, with an average transmission delay of 120 s with a pseudo-random uniform interval between 80–160 s) were surgically implanted in each fish.

Fish were sedated using a Portable Electroanesthesia System (PES™, Smith-Root, Vancouver, WA, USA). The PES™ was set to 100 Hz, 25% duty cycle, and 40 V. Pulsed direct current is appropriate sedation for adult fish because it provides a surgery window of 250–350 s and fish recover quickly with minimal impact to vertebral integrity. Fish were placed supine in a padded V-shaped trough (Vandergoot et al. 2011). Ambient water was continuously pumped over the gills (using a recirculating flow-through pump system) to maintain normal respiration during the surgical period (<5 min). A small incision was made posterior to the pectoral girdle just dorsal of the ventral midline. The acoustic transmitter was inserted posteriorly into the peritoneal cavity. The incision was closed with three interrupted sutures (standard surgical knots). Fish were put in the recovery tank and released 10–15 min post-surgery at the tagging location. Surgical procedures were carried out following approved

animal use protocols of Fisheries and Oceans Canada (FWI-ACC-2017-001) and the University of Nebraska-Lincoln (Project ID: 1208). The length, body mass, and sex (where discernible) of the fish were recorded while tagging. By June 2018, 357 Walleye were tagged (271 Females, 58 Males, and 28 unidentified).

Tagged fish were detected by a grid of Vemco VR2W acoustic receivers (47 in Section 1, 61 in Section 2, and 51 in Section 3) deployed near the bottom of Lake Winnipeg and its major tributaries (Red River and Winnipeg river). In the rivers, distances between receivers varied between 5 and 30 km. In the lake, the receivers were placed on a systematic grid varying between 5 km in the southern part of the south basin and 7 km for the rest of the south basin and narrows, and 14 km in the southern part of the north basin (Fig. 1). A feasibility study on the receiver array can be found in Kraus et al. (2018). Under good acoustic conditions, receivers detect the tag transmission up to 3 km and the probability of detecting a fish by a receiver decreases the further a fish is from the receiver (Fig. 2).

Classical approaches to movement path reconstruction

The simplest approach to reconstruct fish movement paths is to calculate the average locations of the fish at regular time intervals with the weighted average method (Simpfendorfer et al. 2002). For this approach, regular time bins are defined and the number of detections counted for each receiver and each time bin. If $\{\bar{x}_{E,n}, \bar{x}_{N,n}\}$ is the average location (easting and northing respectively) at the n^{th} time bin, then the average locations are obtained as

$$\bar{x}_{E,n} = \frac{\sum_{j=1}^{\mathrm{K}} \mathrm{R}_{n,j} x_{E,j}}{\sum_{j=1}^{\mathrm{K}} \mathrm{R}_{n,j}}, \qquad \bar{x}_{N,n} = \frac{\sum_{j=1}^{\mathrm{K}} \mathrm{R}_{n,j} x_{N,j}}{\sum_{j=1}^{\mathrm{K}} \mathrm{R}_{n,j}}, \tag{1}$$

where $\mathrm{R}_{n,j}$ is the number of detections recorded at the j^{th} receiver within the n^{th} time bin, and $(x_{E,j}, x_{N,j})$ is the location of the j^{th} receiver. K denotes the number of receivers in the array (Simpfendorfer et al. 2002).

Interpolation approaches such as local polynomial regression and kernel estimations (smoothing) can also be used to construct individual movement paths (Hedger et al. 2008). The idea of local polynomial regression is to estimate the underlying smooth function by fitting a series of linear least squares regressions locally. The smoothness of the estimated curve depends on how many neighboring observations are considered in each local regression, this is called the span (k). The selection of neighboring points is usually done symmetrically so that half of neighboring points are at each side of the target point. Friedman's super smoother proposed by Friedman (1984) is an efficient algorithm, that uses a variable span approach with a locally changing span. The optimum local span at each prediction point is selected with cross-validation.

Kernel estimations is similar to local polynomial regression. In kernel estimations, the smoothing is done by calculating local averages while assigning different weights to the neighbors with a kernel. The well-known Gaussian kernel applies more weight to the points closer to the target point and the weights gradually decrease as the points are further away from the target. In their study, Hedger et al. (2008) identified the cross-validated local polynomial regression with Friedman's super smoother (Friedman 1984) to be the optimum

interpolation method, and also recommended kernel estimation with the Gaussian kernel over a box kernel to interpolate fish paths. In this paper, we used the '`sm`' package (Bowman and Azzalini 2018) in '`R`'(R Core Team 2020) to implement the cross-validated local polynomial regression and kernel estimations.

Bayesian state-space models

An SSM contains two sub-models; process model and observation model. This can be expressed as

$$\boldsymbol{x}_t = f(\boldsymbol{x}_{t-1}, \epsilon_t), \tag{2}$$

$$\boldsymbol{y}_t = g(\boldsymbol{x}_t, \eta_t), \tag{3}$$

where $f(.)$ and $g(.)$ represent the process model and the observation model, respectively. Here, $\boldsymbol{x}_t$ is called the latent state and $\boldsymbol{y}_t$ is the observation of the state at time t. In the context of fish movement modeling, $\boldsymbol{x}_t$ represents the true position of the fish that can be in latitude-longitude or Universal Transverse Mercator (UTM) coordinates. $\boldsymbol{y}_t$ represents the observed position, which is usually subjected to errors. The errors associated with each model are denoted by ϵ_t and η_t (Patterson et al. 2008).

Due to the complex nature of SSMs, analytical solutions for the parameters are usually not feasible. One alternative is to use the Bayesian Markov Chain Monte Carlo (MCMC) approach. In the MCMC approach, the initial values of the true position and the model parameters are sequentially updated so that the values of the current step are updated conditioning on the values of the previous step. The simulation is continued until the parameter

estimates converge (Patterson et al. 2008). One of the advantages of using the Bayesian MCMC approach is the ability to incorporate past knowledge about parameters to the models through prior distributions (Jonsen et al. 2003). However, the Bayesian MCMC approach can be very computationally intensive as the SSM becomes more complex.

Constraining the paths

When using SSMs to reconstruct fish paths, it is important to avoid biologically impossible locations. Hence, we have to constrain the model so that the fish trajectory stays within feasible habitats. In our case, the predicted path should remain in the lake or rivers inflowing to the lake. Due to the limited functionality of Bayesian modeling programs such as `'BUGS'` and `'JAGS'`, constraining models is usually very problematic (Plummer et al. 2003; Spiegelhalter et al. 2003). One of the solutions to this problem is the methodology known as the "One's trick" among the `'BUGS'` and `'JAGS'` community. "One's trick" is usually used to specify distributions that have not yet been implemented as a standard distribution in those programs.

Model selection

The deviance information criterion (DIC) suggested by Spiegelhalter et al. (2002), is one of the most widely used measures of predictive accuracy in Bayesian model selection. DIC can be described as the Bayesian version of the Akaike information criterion (AIC) (Gelman et al. 2014) that measures the complexity and fit of a model. One of the reasons for the popularity of DIC is the computational convenience, since DIC is already incorporated into

the 'BUGS' and 'JAGS' packages (Plummer et al. 2003; Spiegelhalter et al. 2003).

State space model implementation

Six Walleye with visibly different behavioural patterns were chosen for the modeling among the 100 inspected to test the methodology. Out of the selected fish, three stayed in the south basin for the entire year and the other three migrated between the south and north basins. The four female fish were larger in size than the two male fish (Table 1). The detection records during the period of June 1^{st}, 2017, to May 31^{st}, 2018, were considered for the movement path reconstruction to study the fish behaviour for the entire year. The detection paths were constructed by connecting the subsequent receiver locations, where the fish was detected (Fig. 3). Each point in Fig. 3 represents a detection, and the true location of the fish can be anywhere within the detection range of the receiver.

The detection records in our data set are in irregular time intervals. Hence, we made them regular by counting the number of detections recorded by each receiver within regular 3 h time bins. Data pooled into 3 h bins reduced the computing burden, and enabled us to estimate fish paths with enough resolution to study any behavioural changes within the day.

The process model

The simplest natural process model we can consider for fish movement is the random walk based on continuous turning angles and step lengths. The true position of the fish (which is unknown) at time t is given by $\boldsymbol{x}_t = \{x_{E,t}, x_{N,t}\}$, are in UTM coordinates. Since UTM coordinates are in meters, it is convenience to calculate distances and areas using the UTM

coordinate system. The process model is given by

$$x_{E,t+1} = x_{E,t} + l_t \sin(\Phi_t), \qquad (4)$$

$$x_{N,t+1} = x_{N,t} + l_t cos(\Phi_t), \qquad (5)$$

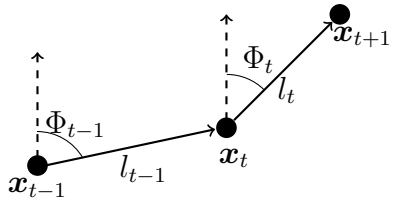

where l_t and Φ_t represent the step length and the turning angle at time t. We considered two scenarios for the distribution of l_t.

$$\text{Scenario 1:} \qquad l_t \sim N(\mu_l, 1/\tau_l), \qquad (6)$$

$$\text{Scenario 2:} \qquad l_t \sim P\phi(\mu_1, \sigma_1^2) + (1-P)\phi(\mu_2, \sigma_2^2). \qquad (7)$$

In Scenario 1, we considered the step lengths to arise from a single Gaussian distribution with parameters μ_l and τ_l, which represent the average step size and the precision (reciprocal of the variance) of the distribution of step size (l_t), respectively. The prior distribution for μ_l was set to be uniform and the prior for τ was set to be non-informative $Gamma(0.1, 0.1)$ based on swimming performance information for Walleye by Peake et al. (2000). In the second scenario, l_t was assumed to follow a Gaussian mixture distribution. Here, $\phi(.)$ denotes the Gaussian density and P defines the mixing probability, where μ_1 and μ_2 are the average step length sizes of the two mixing distributions and σ_1, σ_2 are the standard deviations of corresponding distributions. The ideology behind using the mixture distribution is that fish change their movement behaviour with two-step length distributions at any time step with the probability P. The prior distributions of μ_1 and μ_2 were set to be $Unif(0, 9000)$. The prior for σ_1 and σ_2 were set to be $Unif(0, 100000)$. The $Unif(0, 1)$ was used as the prior for P. The values for the hyper-parameters of μ_1 and μ_2 were defined with the information in the literature (Peake et al. 2000). For both cases, the turning angle was assumed to be

uniformly distributed as below.

$$\Phi_t \sim Unif(-\pi, \pi). \tag{8}$$

The scenario, which resulted in the lowest DIC scores in the final model, was selected as the best model.

The observation model

The second part of the SSM is the observational model, that describes the probability of detection at each receiver at a given time. To model detection probabilities, we used several non-linear functions which have been used in the literature for acoustic telemetry studies (Clark 2016; How and de Lestang 2012). The functions that resulted in the best fit for the observed data are given below. The distance from the true fish position to the j^{th} acoustic receiver at step n is denoted by $d_{n,j}$ and $\pi_{n,j}$ is the detection probability at j^{th} acoustic receiver at step n. Then, the detection probability was estimated with the following four functions:

1. Logistic function

$$log\left(\frac{\pi_{n,j}}{1-\pi_{n,j}}\right) = \alpha_n + \beta_n d_{n,j}, \tag{9}$$

2. Probit function

$$\Phi^{-1}(\pi_{n,j}) = \alpha_n + \beta_n d_{n,j}, \text{ where } \Phi^{-1} \text{ is the inverse cumulative distribution function of the standard distribution,} \tag{10}$$

3. Gaussian kernel function

$$\pi_{n,j} = p_0.e^{-d_{n,j}/2\sigma^2}, \qquad \text{where } p_0 \text{ is the probability of detection at } d_{n,j} = 0, \tag{11}$$

4. Hazard function

$$\pi_{n,j} = p_0 - exp\left(\frac{d_{n,j}}{\beta_1}\right)^{-\beta_2}. \quad (12)$$

The parameters of each model were estimated with the non-linear least squares approach using data from a reference tag experiment in Lake Winnipeg. A line of reference tags was placed in fixed locations with a spacing of 300 m between tags which extends to 3 km from the receiver. The data were obtained under (1) open water and (2) ice-covered conditions (November 9, 2017 to May 10, 2018). Each detection function was fitted for the two data sets separately. Root mean squared error (RMSE), Akaike information criterion (AIC), and Bayesian information criterion (BIC) were calculated for model comparison. The model with minimum error criteria was selected as the observation model for the SSM. Instead of estimating the observation model along with the process model of the SSM, we used the data from the reference tag experiment to estimate the observation model to reduce the computer burden and the variability in the parameter estimates.

Credible intervals for the reconstructed SSM path

The 95% credible intervals were obtained for estimated movement with the SSM approach. Each of the lower bounds were constructed with the 2.5% percentile values of the posterior distributions of x coordinates and y coordinates for the predicted location at each time bin. The upper bounds were obtained similarly with the 97.5% percentile values of the corresponding posterior distributions. Some path segments of the credible intervals constructed in this manner fell outside the lake in the north basin and the narrows. This can be explained by how we defined the lower and upper credible intervals. Each of the lower bounds

were constructed with the 2.5% percentile values of the univariate posterior distributions of x coordinates and y coordinates separately. Even though all the estimated locations in MCMC simulation are constrained inside the lake, lower and upper paths constructed with univariate percentiles can still fall outside the lake. Hence, the credible intervals at each time step (n) were truncated at the lake boundary along a straight line from the average location at time step t and the upper or lower bound that fell outside the lake. In addition, to better understand the movements of each fish, a posterior density plot was created with a sample of points from the posterior densities of fish locations at each time step.

Model estimation

Model estimation was conducted using the Bayesian MCMC approach with '`JAGS`' in R using the package '`R2jags`' (Su and Yajima 2015). The "One's Trick" was used inside the model definition to truncate the conditional distributions at each time step to retain the movement paths in water. To determine if the current location is on land or water, we provided a habitat mask that has a 2 km resolution, which was defined in '`R`' and then provided to '`JAGS`' (Meredith 2013). We then fitted the SSM, by keeping α_n and β_n values fixed in (11). First 10,000 iterations were ignored as burn-in, and thinning was done by selecting each 10^{th} iteration to avoid possible autocorrelation in the converged series.

Movement path analysis

Once the fish movement paths were estimated, movement ecology metrics (step length, turning angle, path length, displacement, tortuosity, and residence time) were used to describe

them (Seidel et al. 2018). Step length describes the distance that fish traveled during each consecutive locations, and the turning angle measures the difference in the two consecutive headings (the direction). The path length is the total distance that fish traveled (or the sum of step sizes). The distribution of step length and turning angle can be used to compare the behavioural changes over time. Displacement measures the "straight-line distance" between the first point and the last point of a fish movement path. Tortuosity measures the wiggliness of the movement paths, that can be measured with either the straightness index or the sinuosity index. The straightness index is used when the movement path is oriented, and the sinuosity index is used otherwise (Benhamou 2004). Sinuosity index is defined as

$$\text{Sinuosity index} = \frac{\sigma_\Phi}{\sqrt{l}}, \tag{13}$$

where σ_Φ is the standard deviation of turning angles, and l is the constant step length. In our reconstructed movement paths, the step lengths were random. Hence, we discretized the trajectory with the '`adehabitatLT`' package in '`R`' (Calenge 2011) to obtain a trajectory with a constant step size. The parameter σ_Φ was estimated with the standard deviation of the turning angles of the estimated path. For each fish, the residence time was calculated for three sections of the lake (Fig. 1).

Simulation Study

To evaluate the performance of the different modeling approaches in estimating the movement paths, we performed a simulation study. The study area was assumed to be a rectangle 32 km wide and 120 km long. First, we simulated ten fish paths inside the study area for 30 d with 2 min time increments, which corresponds to the average transmission delay of

the 'Vemco V16-4H' acoustic transmitters. The receiver array for the simulation study was designed to mimic the real receiver array with increasing distances between receivers from south to north (Fig. 4). The array consists of 73 receivers in total with 42 receivers in the south that are 5 km apart, 25 receivers in the middle 7 km apart, and 6 receivers in the north 14 km apart. Also, we allowed an area with no receivers in the north. The detection probabilities were determined by the logistic function with parameters estimated with data from the reference tags representative of the ice-off period. Paths were estimated under nine settings with combinations of the three time bins (3 h, 6 h, 12 h) and three different lengths of tracking periods (10 d , 20 d, 30 d). The true simulated average paths were also obtained for each time bin and tracking period, using true simulated paths. To evaluate the accuracy of each reconstructed path, the root-mean-squared error between the true average path and the reconstructed path was calculated for the total distance traveled and the tortuosity.

Results

Simulation Study

By visual inspection, we noticed that except for the paths reconstructed with cross-validated local polynomial regression method, all other reconstruction paths gave satisfactory results in estimating true paths (Fig. 5). Cross-validated local polynomial regression paths were over smoothed and lost most of the true movement patterns. The weighted average paths and the kernel smoothing paths appeared similar. Furthermore, the SSM approach reconstructed some of the path segments even for the areas with no receivers. We observed that the SSM

method resulted in lower RMSE values of total distance except for Simulation 3 where the bin size was the largest and the tracking period was the lowest (Table 2). Also, the SSM approach gave lower RMSE values for tortuosity for a longer tracking period with lower bin sizes. In addition, we calculated the residence times for all movement paths under each simulation setting with respect to three sections in the study area (Table 3). However, except for the cross-validated local polynomial regression, all the reconstruction methods estimated the true residence time accurately in almost all cases. In most cases, the SSM method resulted in slightly lower RMSE values for residence time than the simple weighted average and kernel smoothing methods.

Movement path reconstruction

The estimated detection curves with logistic and probit functions were almost identical (Fig. 2) with the lowest errors (Table 4). Hence, we selected the logit model as the detection function for the state space model.

For "Wall-001" and "Wall-007", the model with mixture step length distribution (Scenario 2) gave lower DIC scores while other fish paths favour the model having step lengths with a normal distribution (Scenario 1). Hence, in the proceeding sections, for each fish, the SSM path refers to the reconstructed paths with the SSM approach using the best scenario that resulted in the minimum DIC (Table 5).

For all fish, the weighted average paths constructed with 3 h time bins and the kernel smoothing paths with 3 h bandwidth, appeared almost identical (Fig. 6, Fig. 7). Cross-

validated local polynomial regression paths were most smoothed, and do not provide any insight about the individual movement paths. Furthermore, all three smoothing methods predicted some path sections on land, which is unfavorable. However, the SSM approach resulted in movement paths that were constrained within the lake except for few path segments through islands and narrows. It is important to note that the SSM path is an average path that was constructed by connecting the means of the univariate posterior distributions of x coordinates and y coordinates at each time bin. Hence, when the simulated points at a certain time step are distributed around an island or an edge, the average of the posterior distribution can fall on the island.

In the lower part of the south basin of the lake, where the resolution of the grid of receivers is high, the 95% credible intervals for the SSM path did not deviate much from the average path (Fig.s 8 and Fig. 9). However, in the narrows and the north basin, the predicted paths were unstable and subject to high variation due to the low resolution of the receiver array. In some cases, we noticed that the posterior density around certain points was lower than their neighboring area. This can be seen as some light dots in the middle of dark areas (Fig.s 8 and Fig. 9). This occurred around some receivers, which did not detect the fish for a certain period of time. In this case, the Markov chain avoided simulating fish positions near those receivers.

Movement path analysis

The metrics for the weighted average paths and the kernel smoothing paths were very similar (Table 6 and Table 7). Due to the highly smoothed nature of the cross-validated local

polynomial regression method, the metrics of those paths differed significantly from the SSM paths and other smoothed paths. It gives lower path lengths and tortuosity values than the other methods. For some fish, the path lengths for the SSM models were considerably larger than the path lengths for other smoothing approaches. Except for the cross-validated local polynomial regression approach, tortuosity values and residence times for all the approaches were similar (Table 6 and Table 7).

When there was no detection for a certain period or the fish was continuously detected by the same receiver for an extended period, the weighted mean method and other smoothing approaches failed to predict any fish movements. For the entire period that the fish was unobserved, the estimated step lengths was zero and there was no any information on turning angles. However, the SSM approach predicted some fish movements even when there was no detection. This was clearly visible in the reconstructed paths for "Wall-001" (Fig. 6). The SSM approach showed three path segments between the Hecla and Gimli area while other approaches predicted a single path. When fish moved north, it was detected by receivers and all the reconstructed approaches were able to estimate the path segment. Once the fish returned to the Gimli region, it was undetected for about two months in the winter. Hence, the smoothing approaches failed to estimate the path. However, the SSM approach still predicted a probable path segment based on the process model by borrowing information across regions.

In the case that the fish was detected by the same receiver for an extended period, the SSM approach did not assume that the fish stayed still as the smoothing methods do, and it predicted small movements around the receiver based on the underlying process model. This

property allowed the SSM approach to produce more realistic paths that resulted in higher path lengths. This was clearly noticeable for the fish that migrated to the north basin where the receiver density was lower.

Discussion

We reconstructed movement paths of tagged Walleye using detection records from the grid of acoustic receivers and analyzing the data by applying different classical smoothing techniques and Bayesian SSMs. In the SSM approach, we used a simple random walk model with normally distributed step lengths, and a Gaussian mixture to account for complex behavioural changes in fish movements (behavioural states) over time. Using DIC criteria, we selected the best SSM model for each fish. All the smoothing methods predicted some path sections on land while the estimated SSM paths were well constrained within the lake. The SSM approach also estimated the unobserved fish movement paths to some extent even with missing detections for a few weeks or portions of the north basin with no receivers, by borrowing information from data-rich regions. This is not possible with classical smoothing techniques. Also, for SSMs, we incorporated available prior knowledge such as information on detection probabilities including temporal changes and swimming speed, to define suitable prior distributions and their parameters. Through simulation studies, we confirmed that the SSM approach can estimate ecological movement metrics with slightly better accuracy than the classical approaches, especially when using smaller time bins and longer tracking periods.

The presented SSM can easily be modified with different process models. If the fish move-

ment paths show persistence in the movement direction, rather than using uniform turning angles, it is better to use wrapped normal, wrapped Cauchy, or Von Mises distribution with zero expectation (Codling et al. 2008) as the distribution of turning angles. Before settling with the process models that we presented in this paper, we explored the possibility of using more complex movement models such as the OU process, that accounts for any attraction towards spatially varying local home range centers following the work by Alós et al. (2016). However, the reconstructed paths showed a huge attraction towards the home range centers, that could not be justified by Walleye biology. Also, the large number of parameters in the OU process-based model caused a significantly higher computing burden in the estimation process compared to the random walk based model. When fish paths show different movement behaviour patterns (behavioural states) at different times, the multi-state random walk model suggested by Nicosia et al. (2017) may be a potential alternative to the Alós et al. (2016) approach.

Hostetter and Royle (2020) presented a similar framework to the SSM approach to estimate animal locations using acoustic telemetry data with the assistance of a simple Gaussian Markov process model and an observation model that was estimated with observed data. However, estimating the observation model inside the SSM framework would add an additional computing burden and might result in convergence issues. Hence, we recommend estimating the detection functions using a reference tag experiment whenever possible. The frameworks presented by Alós et al. (2016),Breed et al. (2017),Pedersen and Weng (2013), and Hostetter and Royle (2020) seem to work well for small scale systematic acoustic telemetry studies that monitor a small region (i.e., a few km^2) with a few receivers with overlapping

detection ranges. For large-scale movement tracking where the receiver grid has been spread over a large area (i.e., hundreds or thousands of km^2) non-uniformly with non-overlapping detection ranges, the use of complex models such as SSMs is challenging. In our study, using real data from a large-scale telemetry study and through a comprehensive simulation study, we compared the performance of classical approaches and the SSM approach in predicting unobserved fish movements. Furthermore, none of the aforementioned papers provided a framework to constrain the reconstructed paths inside the plausible area. In this paper, we illustrated how to constrain the the reconstructed paths with widely used Bayesian MCMC sampler JAGS to maintain the model inside a complex shaped habitat.

The main limitation of the SSM approach is the high computing burden. For instance, to fit a model for a single Walleye with the Bayesian MCMC approach, it took around nine hours on Compute Canada Béluga computer facility (CPUs: Intel Gold 6148 Skylake @ 2.4 GHz). Hence, one has to maintain a trade-off among multiple factors including the model complexity, tracking period, time frequency, and computing burden. Due to these reasons, we had to limit our simulation study to a few settings with fewer time steps. Another issue with modeling Walleye movement paths with our data was the high uncertainty of the paths for the regions where the resolution of the acoustic grid was lower. However, due to cost and other practical concerns, maintaining a higher resolution throughout a large water body such as Lake Winnipeg is difficult.

Reconstructed paths can be used to answer important questions related to Walleye in Lake Winnipeg. For instance, do the fish that migrate to north basin move differently than fish that stay in the south basin? If they move differently, is this putting a portion of the

population at risk relative to the other fish? For example, a Walleye that occupies the area along the shore is at higher risk due to commercial and recreational fishing activities compared to a fish that occupies off-shore area. Also, those fish that travel longer distances have a higher chance to encounter a fishing net than the fish that travels less.

Finally, we conclude that SSM is a powerful, yet, sophisticated and computer-intensive tool that can be used to better understand acoustic telemetry data. In addition to the better accuracy in predicting unobserved animal paths, another advantage of using SSMs over smoothing methods is that its ability to quantify the uncertainty associated with estimated animal movement paths. However, classical smoothing methods are still useful to have quick but comparatively accurate estimates for animal moment paths using acoustic telemetry data.

Acknowledgment

The study was funded by Fisheries and Oceans Canada (DFO) Partnership Fund, Fish and Wildlife Enhancement Fund, and the International Joint Commission. Also, we acknowledge our collaborators, Agriculture and Resource Development Manitoba, University of Nebraska, and Lakehead University. Furthermore, we thank the Department of Statistics, Department of Biological Sciences and Graduate Studies of the University of Manitoba for the financial support and assistance. Dr. Gillis and Dr. Muthukumarana have been partially supported by discovery grants from the Natural Sciences and Engineering Research Council of Canada.

References

Albertsen, C. M., Whoriskey, K., Yurkowski, D., Nielsen, A. and Flemming, J. M. (2015), 'Fast fitting of non-gaussian state-space models to animal movement data via template model builder', *Ecology* **96**(10), 2598–2604.

Alós, J., Palmer, M., Balle, S. and Arlinghaus, R. (2016), 'Bayesian state-space modelling of conventional acoustic tracking provides accurate descriptors of home range behavior in a small-bodied coastal fish species', *PloS one* **11**(4), e0154089.

Benhamou, S. (2004), 'How to reliably estimate the tortuosity of an animal's path:: straightness, sinuosity, or fractal dimension?', *Journal of theoretical biology* **229**(2), 209–220.

Bolker, B. M. (2008), *Ecological models and data in R*, Princeton University Press.

Bowman, A. W. and Azzalini, A. (2018), *R package* `sm`*: nonparametric smoothing methods (version 2.2-5.6)*, University of Glasgow, UK and Università di Padova, Italia.
URL: *http://www.stats.gla.ac.uk/ adrian/sm/*

Breed, G. A., Golson, E. A. and Tinker, M. T. (2017), 'Predicting animal home-range structure and transitions using a multistate ornstein-uhlenbeck biased random walk', *Ecology* **98**(1), 32–47.

Brownscombe, J. W., Lédée, E. J., Raby, G. D., Struthers, D. P., Gutowsky, L. F., Nguyen, V. M., Young, N., Stokesbury, M. J., Holbrook, C. M., Brenden, T. O. et al. (2019), 'Conducting and interpreting fish telemetry studies: considerations for researchers and resource managers', *Reviews in Fish Biology and Fisheries* **29**(2), 369–400.

Brunskill, G., Elliott, S. and Campbell, P. (1980), Morphometry, hydrology, and watershed data pertinent to the limnology of Lake Winnipeg, Canadian manuscript report of fisheries and aquatic science no. 1556, Department of Fisheries and Oceans,Winnipeg, Manitoba.

Calenge, C. (2011), 'Analysis of animal movements in r: the adehabitatlt package', *R Foundation for Statistical Computing: Vienna, Austria* .

Clark, R. G. (2016), 'Statistical efficiency in distance sampling', *PloS one* **11**(3).

Codling, E. A., Plank, M. J. and Benhamou, S. (2008), 'Random walk models in biology', *Journal of the Royal society interface* **5**(25), 813–834.

Cooke, S. J., Hinch, S. G., Wikelski, M., Andrews, R. D., Kuchel, L. J., Wolcott, T. G. and Butler, P. J. (2004), Biotelemetry: a mechanistic approach to ecology. trends in ecology, *in* 'Evolution', Citeseer.

Cooke, S. J., Iverson, S. J., Stokesbury, M. J., Hinch, S. G., Fisk, A. T., VanderZwaag, D. L., Apostle, R. and Whoriskey, F. (2011), 'Ocean tracking network canada: a network approach to addressing critical issues in fisheries and resource management with implications for ocean governance', *Fisheries* **36**(12), 583–592.

Cooke, S. J., Martins, E. G., Struthers, D. P., Gutowsky, L. F., Power, M., Doka, S. E., Dettmers, J. M., Crook, D. A., Lucas, M. C., Holbrook, C. M. et al. (2016), 'A moving target—incorporating knowledge of the spatial ecology of fish into the assessment and management of freshwater fish populations', *Environmental Monitoring and Assessment* **188**(4), 239.

Donaldson, M. R., Hinch, S. G., Suski, C. D., Fisk, A. T., Heupel, M. R. and Cooke, S. J. (2014), 'Making connections in aquatic ecosystems with acoustic telemetry monitoring', *Frontiers in Ecology and the Environment* **12**(10), 565–573.

Fisheries and Canada, O. (2020), 'Freshwater landings, 2018', `https://www.dfo-mpo.gc.ca/stats/commercial/land-debarq/freshwater-eaudouce/2018-eng.htm`. [Online; accessed 12-Feb-2021].

Friedman, J. H. (1984), A variable span smoother, Technical report, Stanford Univ CA Lab for Computational Statistics.

Gelman, A., Hwang, J. and Vehtari, A. (2014), 'Understanding predictive information criteria for bayesian models', *Statistics and computing* **24**(6), 997–1016.

Hartman, G. (2009), 'A biological synopsis of walleye (sander vitreus)', *Canadian Manuscript Report of Fisheries and Aquatic Sciences 2888* **v+48p**.

Hedger, R. D., Martin, F., Dodson, J. J., Hatin, D., Caron, F. and Whoriskey, F. G. (2008), 'The optimized interpolation of fish positions and speeds in an array of fixed acoustic receivers', *ICES Journal of Marine Science* **65**(7), 1248–1259.

Hostetter, N. J. and Royle, J. A. (2020), 'Movement-assisted localization from acoustic telemetry data', *Movement Ecology* **8**, 1–13.

How, J. R. and de Lestang, S. (2012), 'Acoustic tracking: issues affecting design, analysis and interpretation of data from movement studies', *Marine and Freshwater Research* **63**(4), 312–324.

Johnston, T. A., Lysack, W. and Leggett, W. C. (2012), 'Abundance, growth, and life history characteristics of sympatric walleye (sander vitreus) and sauger (sander canadensis) in lake winnipeg, manitoba', *Journal of Great Lakes Research* **38**, 35–46.

Jonsen, I. D., Myers, R. A. and Flemming, J. M. (2003), 'Meta-analysis of animal movement using state-space models', *Ecology* **84**(11), 3055–3063.

Klimley, A. P., Voegeli, F., Beavers, S. C. and Le Boeuf, B. J. (1998), 'Automated listening stations for tagged marine fishes', *Marine Technology Society Journal* **32**(1), 94–101.

Klinard, N. V., Halfyard, E. A., Matley, J. K., Fisk, A. T. and Johnson, T. B. (2019), 'The influence of dynamic environmental interactions on detection efficiency of acoustic transmitters in a large, deep, freshwater lake', *Animal Biotelemetry* **7**(1), 17.

Kraus, R. T., Holbrook, C. M., Vandergoot, C. S., Stewart, T. R., Faust, M. D., Watkinson, D. A., Charles, C., Pegg, M., Enders, E. C. and Krueger, C. C. (2018), 'Evaluation of acoustic telemetry grids for determining aquatic animal movement and survival', *Methods in Ecology and Evolution* **9**(6), 1489–1502.

Meredith, M. (2013), 'Secr in bugs/jags with patchy habitat'. `http://mikemeredith.net/blog/1309_SECR_in_JAGS_patchy_habitat.htm`, visited 2019-08-15.

Nicosia, A., Duchesne, T., Rivest, L.-P. and Fortin, D. (2017), 'A general hidden state random walk model for animal movement', *Computational Statistics & Data Analysis* **105**, 76–95.

Patterson, T. A., Parton, A., Langrock, R., Blackwell, P. G., Thomas, L. and King, R. (2017),

'Statistical modelling of individual animal movement: an overview of key methods and a discussion of practical challenges', *AStA Advances in Statistical Analysis* **101**(4), 399–438.

Patterson, T. A., Thomas, L., Wilcox, C., Ovaskainen, O. and Matthiopoulos, J. (2008), 'State–space models of individual animal movement', *Trends in ecology & evolution* **23**(2), 87–94.

Peake, S., McKinley, R. S. and Scruton, D. A. (2000), 'Swimming performance of walleye (stizostedion vitreum)', *Canadian Journal of Zoology* **78**(9), 1686–1690.
URL: *https://doi.org/10.1139/z00-097*

Pedersen, M. W. and Weng, K. C. (2013), 'Estimating individual animal movement from observation networks', *Methods in Ecology and Evolution* **4**(10), 920–929.

Plummer, M. et al. (2003), Jags: A program for analysis of bayesian graphical models using gibbs sampling, *in* 'Proceedings of the 3rd international workshop on distributed statistical computing', Vol. 124, Vienna, Austria., p. 10.

R Core Team (2020), *R: A Language and Environment for Statistical Computing*, R Foundation for Statistical Computing, Vienna, Austria.
URL: *https://www.R-project.org/*

Reubens, J., Verhelst, P., van der Knaap, I., Deneudt, K., Moens, T. and Hernandez, F. (2019), 'Environmental factors influence the detection probability in acoustic telemetry in a marine environment: results from a new setup', *Hydrobiologia* **845**(1), 81–94.

Seidel, D. P., Dougherty, E., Carlson, C. and Getz, W. M. (2018), 'Ecological metrics and

577 methods for gps movement data', *International Journal of Geographical Information Sci-*
578 *ence* **32**(11), 2272–2293.

579 Sheppard, K. T., Davoren, G. K. and Hann, B. J. (2015), 'Diet of walleye and sauger
580 and morphological characteristics of their prey in lake winnipeg', *Journal of Great Lakes*
581 *Research* **41**(3), 907–915.

582 Simpfendorfer, C. A., Heupel, M. R. and Hueter, R. E. (2002), 'Estimation of short-term
583 centers of activity from an array of omnidirectional hydrophones and its use in studying
584 animal movements', *Canadian Journal of Fisheries and Aquatic Sciences* **59**(1), 23–32.

585 Spiegelhalter, D. J., Best, N. G., Carlin, B. P. and Van Der Linde, A. (2002), 'Bayesian
586 measures of model complexity and fit', *Journal of the royal statistical society: Series b*
587 *(statistical methodology)* **64**(4), 583–639.

588 Spiegelhalter, D., Thomas, A., Best, N. and Lunn, D. (2003), 'Winbugs user manual version
589 1.4 january 2003', *Upgraded to version* **1**(3).

590 Stewardship, M. W. et al. (2011), State of lake winnipeg: 1999 to 2007, Technical report,
591 Environment Canada and Manitoba Water Stewardship.

592 Stewart, K. W. and Watkinson, D. A. (2004), *The freshwater fishes of Manitoba*, Univ. of
593 Manitoba Press.

594 Su, Y.-S. and Yajima, M. (2015), *Package 'R2jags'*. Available at `http://CRAN.R-project.`
595 `org/package=R2jags`, version 0.5-7.

596 Thorstensen, M. J., Wiens, L. M., Jeffrey, J. D., Klein, G. M., Jeffries, K. M. and Treberg,

J. R. (2020), 'Morphology and blood metabolites reflect recent spatial and temporal differences among lake winnipeg walleye, sander vitreus', *Journal of Great Lakes Research* .

Vandergoot, C. S., Murchie, K. J., Cooke, S. J., Dettmers, J. M., Bergstedt, R. A. and Fielder, D. G. (2011), 'Evaluation of two forms of electroanesthesia and carbon dioxide for short-term anesthesia in walleye', *North American Journal of Fisheries Management* **31**(5), 914–922.

Wassenaar, L. I. and Rao, Y. R. (2012), 'Lake winnipeg: The forgotten great lake', *Journal of Great Lakes Research* **38**, 1–5.

Wickham, H. (2016), *ggplot2: Elegant Graphics for Data Analysis*, Springer-Verlag New York.

URL: *https://ggplot2.tidyverse.org*

Table 1: Biological information of the the six Walleye selected for testing the modeling approach for the movement path reconstruction.

Fish ID	Gender	Body mass (kg)	Fork length (mm)	No. of detections
Wall-001	Male	2.25	572	60 940
Wall-004	Female	3.80	678	63 828
Wall-006	Female	3.55	630	35 940
Wall-007	Male	1.45	519	58 030
Wall-010	Female	3.30	640	68 015
Wall-032	Female	5.15	711	30 776

Table 2: RMSE values of path lengths and tortuosity for simple weighted average method (WA), kernel smoothing with the Gaussian kernel (KS), cross-validated local polynomial regression approach (LPR), and the state-space modelling approach (SSM) under different simulation settings.

Simulation	Number of days	Bin size (hrs)	RMSE - Path length (km)				RMSE - Tortuosity			
			WA	LPR	KS	SSM	WA	LPR	KS	SSM
1	10	3	0.0390	0.1175	0.1094	0.0481	55.82	204.53	97.11	51.70
2	10	6	0.0417	0.1015	0.0426	0.0353	28.08	98.22	59.99	24.60
3	10	12	0.0382	0.0783	0.0782	0.0563	10.79	33.97	42.54	17.83
4	20	3	0.0571	0.1857	0.0674	0.0519	177.45	541.90	218.95	168.54
5	20	6	0.0483	0.1418	0.0623	0.0396	96.70	299.41	137.36	88.42
6	20	12	0.0388	0.0938	0.0435	0.0365	62.78	144.55	109.62	59.31
7	30	3	0.0631	0.2229	0.0720	0.0450	312.18	888.72	376.12	271.20
8	30	6	0.0433	0.1633	0.0688	0.0421	187.38	526.76	242.32	158.06
9	30	12	0.0310	0.1223	0.0265	0.0330	117.22	291.84	170.55	100.97

Table 3: RMSE values of residence time (as a proportion of the total time) at three sections of the study area for simple weighted average method (WA), kernel smoothing with the Gaussian kernel (KS), cross-validated local polynomial regression approach (LPR), and the state-space modelling approach (SSM) under different simulation settings.

Simulation	No of days	Bin size (h)	Section 1 (Y<40 km)				Section 2 (40 km<Y<80 km)				Section 3 (Y>80 km)			
			WA	LPR	KS	SSM	WA	LPR	KS	SSM	WA	LPR	KS	SSM
1	10	3	0.0438	0.0333	0.0387	0.0181	0.0444	0.0505	0.0397	0.0240	0.0040	0.0373	0.0125	0.0158
2	10	6	0.0306	0.0296	0.0512	0.0250	0.0345	0.0518	0.0530	0.0306	0.0158	0.0426	0.0177	0.0177
3	10	12	0.0224	0.0158	0.0316	0.0224	0.0224	0.0387	0.0316	0.0224	0.0000	0.0354	0.0000	0.0000
4	20	3	0.0276	0.0262	0.0243	0.0128	0.0307	0.0926	0.0270	0.0140	0.0114	0.1719	0.1484	0.0084
5	20	6	0.0153	0.0250	0.0377	0.0158	0.0271	0.0980	0.0458	0.0227	0.0224	0.1738	0.1476	0.0163
6	20	12	0.0079	0.0158	0.0418	0.0112	0.0137	0.0829	0.0447	0.0158	0.0112	0.1622	0.1510	0.0112
7	30	3	0.0310	0.0385	0.0301	0.0062	0.0412	0.0605	0.0336	0.0113	0.0215	0.1560	0.1416	0.0116
8	30	6	0.0179	0.0401	0.0387	0.0149	0.0376	0.0681	0.0465	0.0269	0.0300	0.1578	0.1425	0.0220
9	30	12	0.0118	0.0253	0.0435	0.0118	0.0269	0.0503	0.0447	0.0204	0.0242	0.1528	0.1442	0.0167

Table 4: The error measurements for different detection functions.

Model	Open water			Ice Covered		
	RMSE	AIC	BIC	RMSE	AIC	BIC
Logit	0.0338	-33.38	-32.47	0.0932	-13.07	-12.16
Probit	0.0340	-33.23	-32.32	0.0918	-13.39	-12.49
Gaussian kernel	0.0351	-32.63	-31.73	0.0977	-12.14	-11.23
Hazard	0.0362	-29.97	-28.76	0.0975	-10.18	-8.97

Table 5: DIC scores for fitted models. For each fish, model with the lower DIC was selected as the best SSM (marked with *) to reconstruct the movement paths. ΔDIC is the difference in the DIC scores for the models under two scenarios.

Fish ID	Wall-001	Wall-004	Wall-006	Wall-007	Wall-010	Wall-032
Scenario 1	92954.2	*110287.0	*35757.0	134017.6	*90910.9	*42822.5
Scenario 2	*92948.5	110355.2	35878.2	*134011.6	91125.2	42902.5
ΔDIC	5.7	68.2	121.2	6.0	214.3	80.0

Table 6: Path lengths and tortuosity for simple weighted average method (WA), kernel smoothing with the Gaussian kernel (KS), cross-validated local polynomial regression approach (LR), and the state-space modelling approach (SSM) for six selected Walleye.

Fish ID	Path length (km)				Tortuosity			
	WA	LR	KS	SSM	WA	LR	KS	SSM
Wall-001	1,336	343	1,305	1,643	0.0175	0.0082	0.0163	0.0167
Wall-004	1,724	194	1,691	1,592	0.0213	0.0140	0.0211	0.0209
Wall-006	1,417	405	1,437	1,620	0.0175	0.0105	0.0184	0.0168
Wall-007	1,688	231	1,688	1,668	0.0203	0.0111	0.0206	0.0217
Wall-010	1,550	191	1,583	1,549	0.0225	0.0181	0.0227	0.0221
Wall-032	1,370	419	1,376	1,752	0.0192	0.0113	0.0189	0.0186

Table 7: Residence time (as a proportion of the total time) at three sections of the lake for simple weighted average method (WA), kernel smoothing with the Gaussian kernel (KS), cross-validated local polynomial regression approach (LR), and the state-space modelling approach (SSM) for six selected Walleye.

Fish ID	Section 1				Section 2				Section 3			
	WA	LR	KS	SSM	WA	LR	KS	SSM	WA	LR	KS	SSM
Wall-001	0.1083	0.0902	0.1083	0.1086	0.5489	0.5645	0.5482	0.5475	0.3428	0.3452	0.3435	0.3439
Wall-004	0.3326	0.3646	0.3428	0.3435	0.6674	0.6354	0.6572	0.6565	0	0	0	0
Wall-006	0.4921	0.4959	0.4928	0.4948	0.2717	0.2631	0.271	0.2672	0.2362	0.241	0.2362	0.2379
Wall-007	0.099	0.0983	0.1069	0.1089	0.901	0.9017	0.8931	0.8911	0	0	0	0
Wall-010	0.0354	0.0079	0.0354	0.0347	0.8863	0.9763	0.886	0.886	0.0783	0.0158	0.0786	0.0793
Wall-032	0.5943	0.5836	0.5957	0.5967	0.2425	0.2734	0.2418	0.2401	0.1632	0.1429	0.1625	0.1632

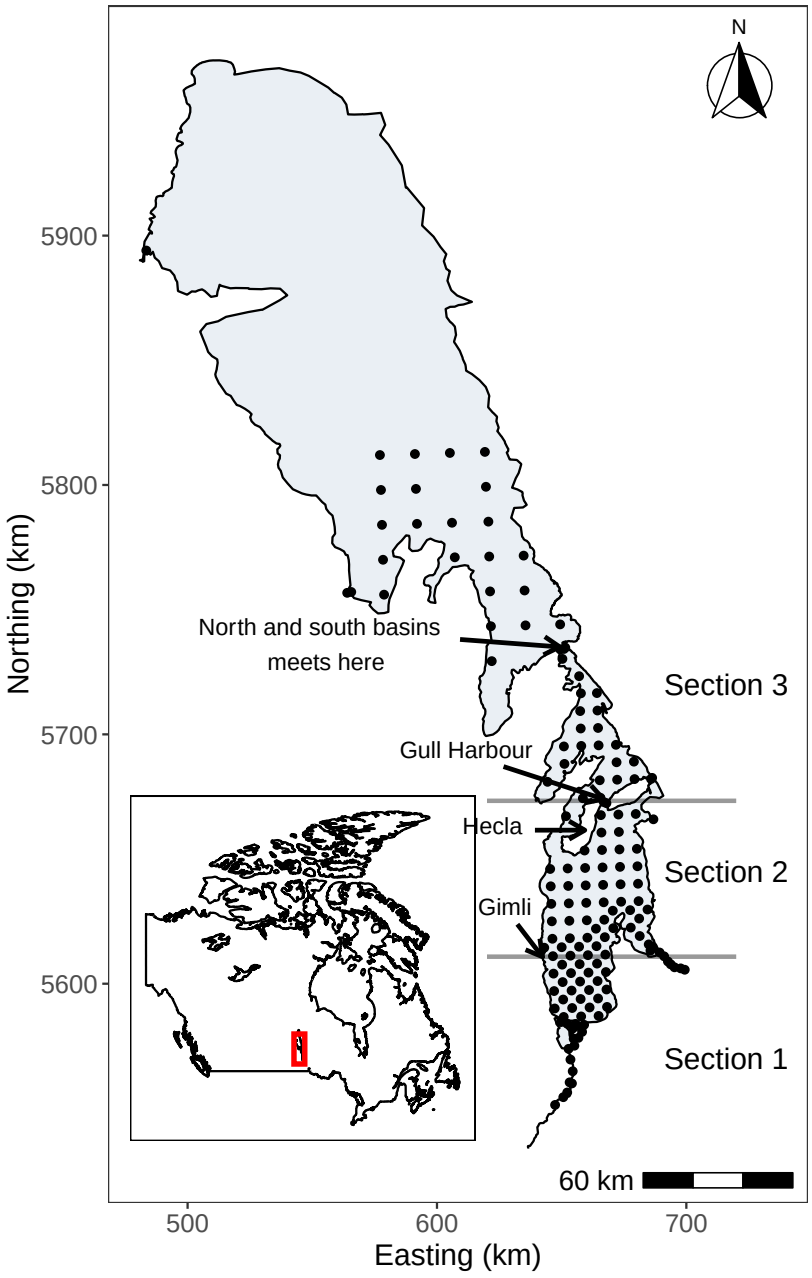

Figure 1: Lake Winnipeg and the locations of the acoustic receivers indicated by '•'. The study area was divided into three sections. Section 1 is the area south of Gimli, Section 2 is the area between Gimli and Gull Harbour, and Section 3 is the area north of Gull Harbour. Map was made using R with ggplot2.

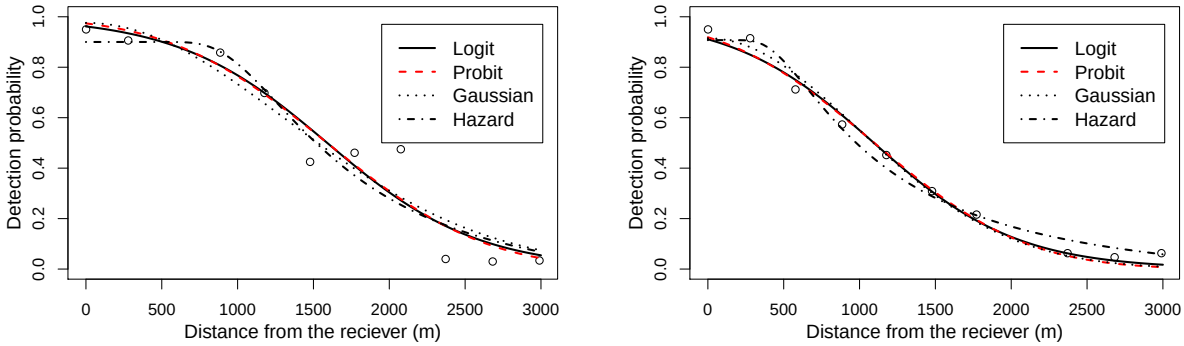

(a) Ice covered.

(b) Open water.

Figure 2: Detection data and estimated detection functions. The curves were estimated separately for open-water data and ice-covered data.

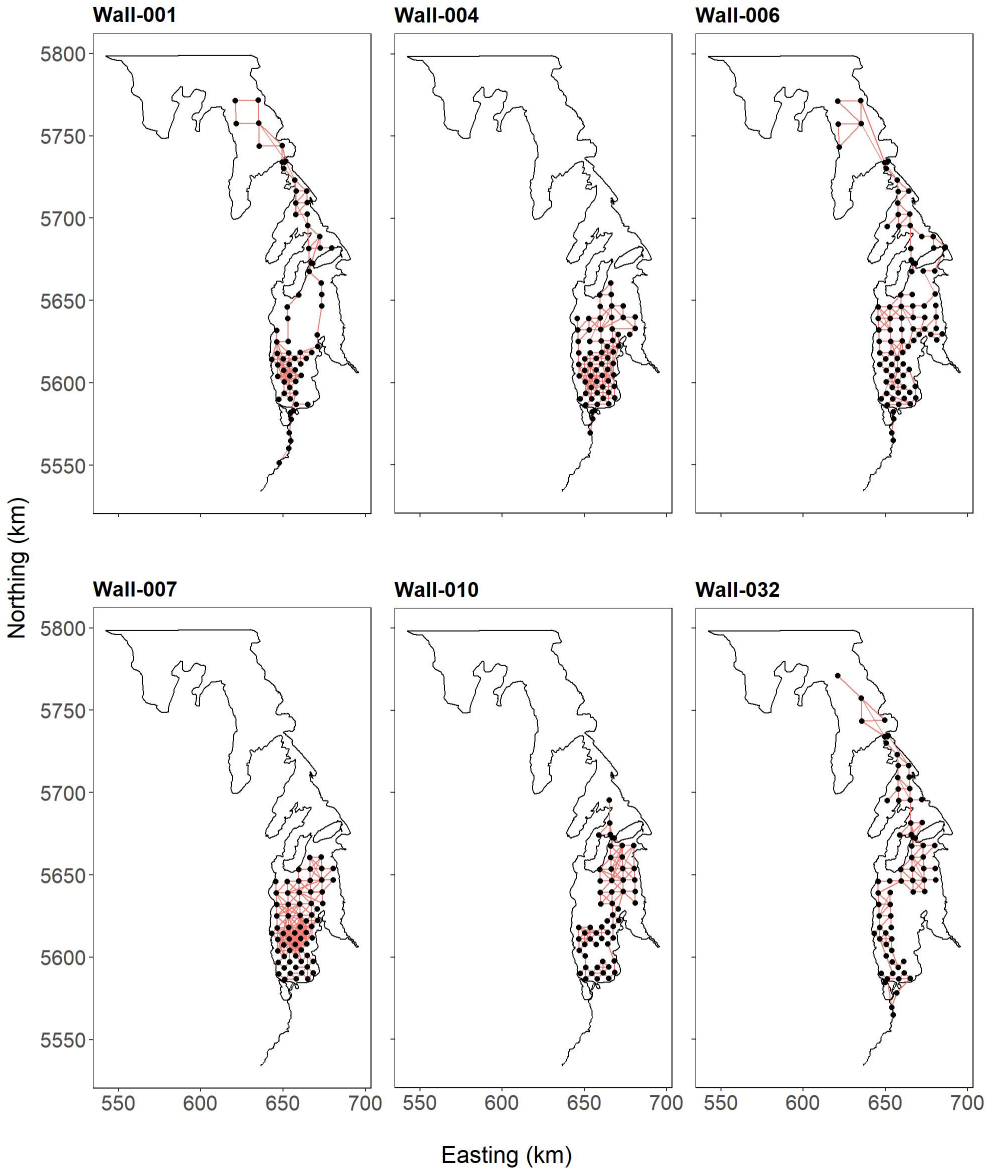

Figure 3: Detection paths for six selected Walleye that were constructed by connecting the consecutive receiver locations where fish were detected. Maps were made using R with ggplot2.

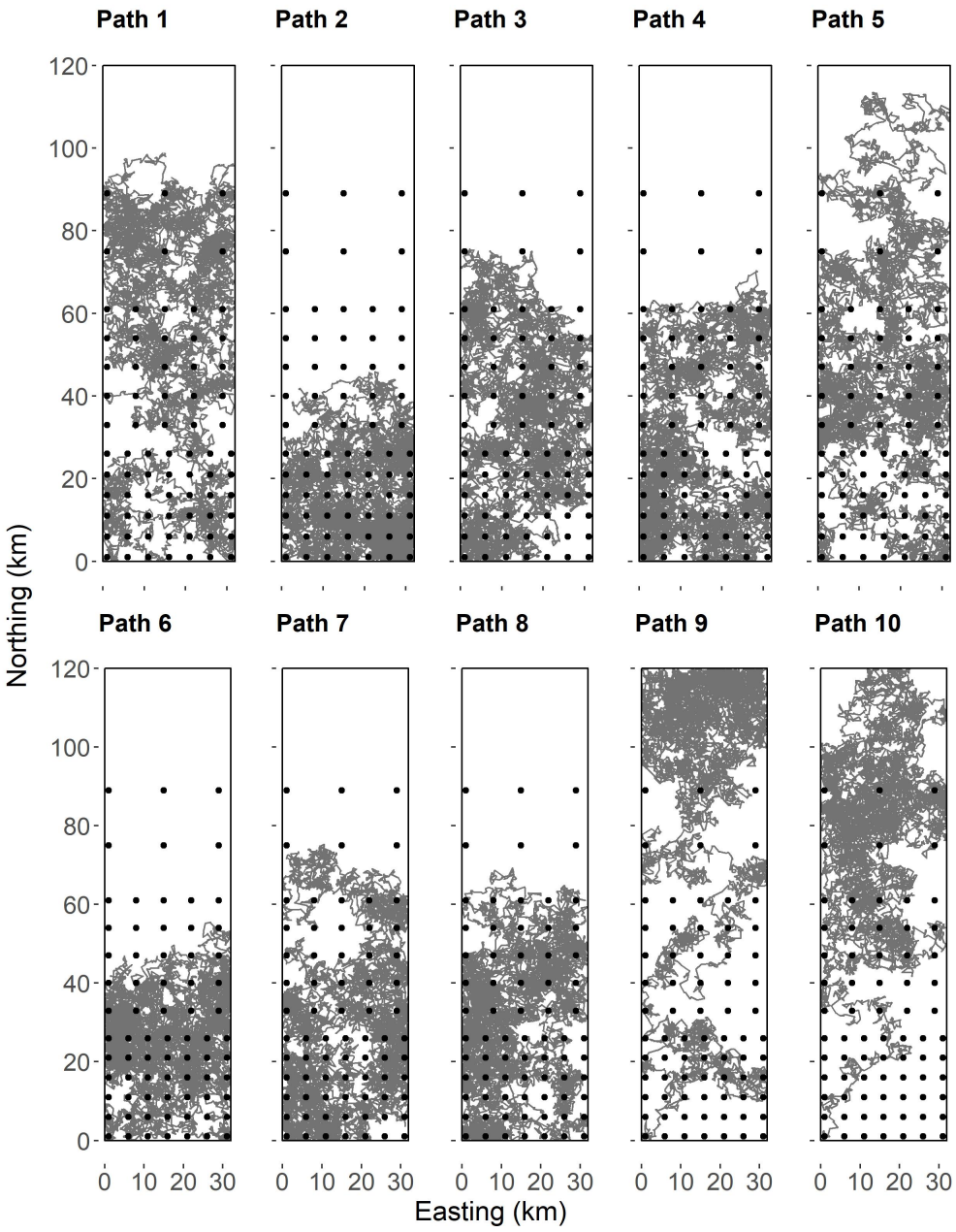

Figure 4: Simulated trajectories for 30 d with 2 min time increments. The receiver locations are denoted by '•'. The spacing between the receivers changes from the bottom to top (4 km, 7 km, and 14 km).

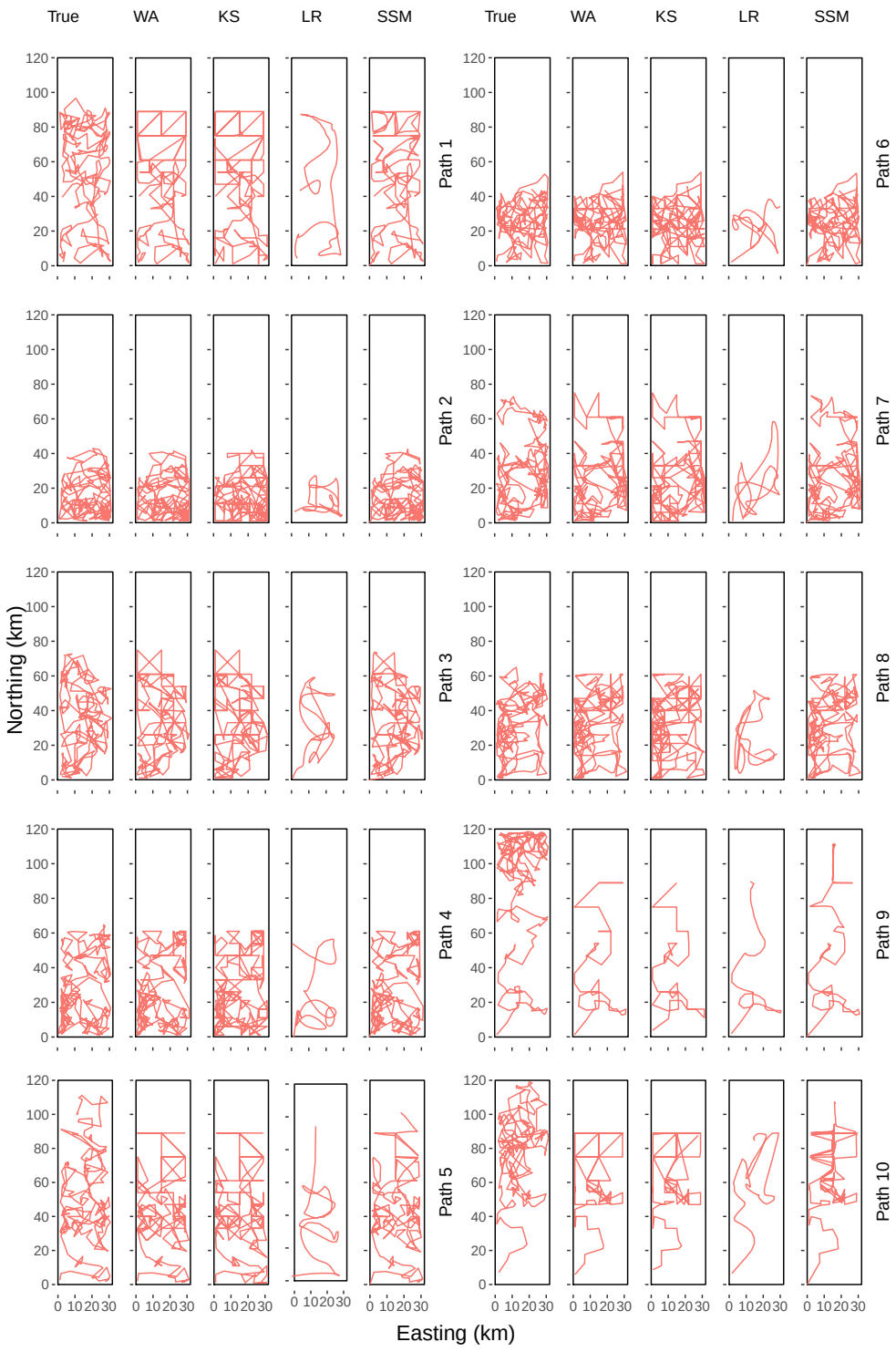

Figure 5: The true average path using 3 h time bins (True), reconstructed movement paths with the simple weighted average method (WA), kernel smoothing with the Gaussian kernel (KS), cross-validated local polynomial regression approach (LR), and the state-space modeling approach (SSM) for Simulation 7 (time bin = 3 h and tracking period = 30 d).

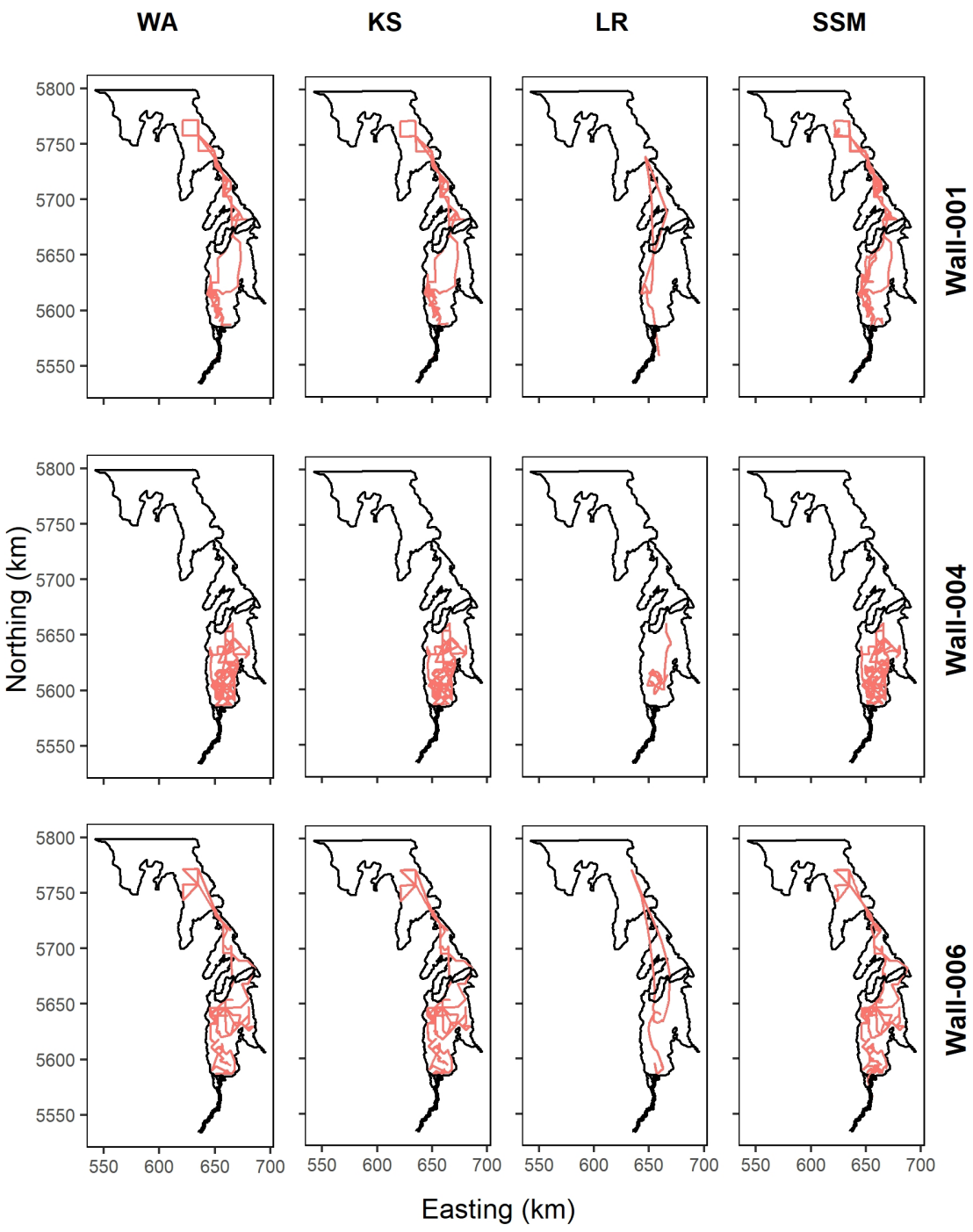

Figure 6: Reconstructed movement paths with the simple weighted average method (WA), kernel smoothing with the Gaussian kernel (KS), cross-validated local polynomial regression approach (LR), and the state-space modeling approach (SSM) for the fish "Wall-001", "Wall-004", and "Wall-006". Maps were made using R with ggplot2.

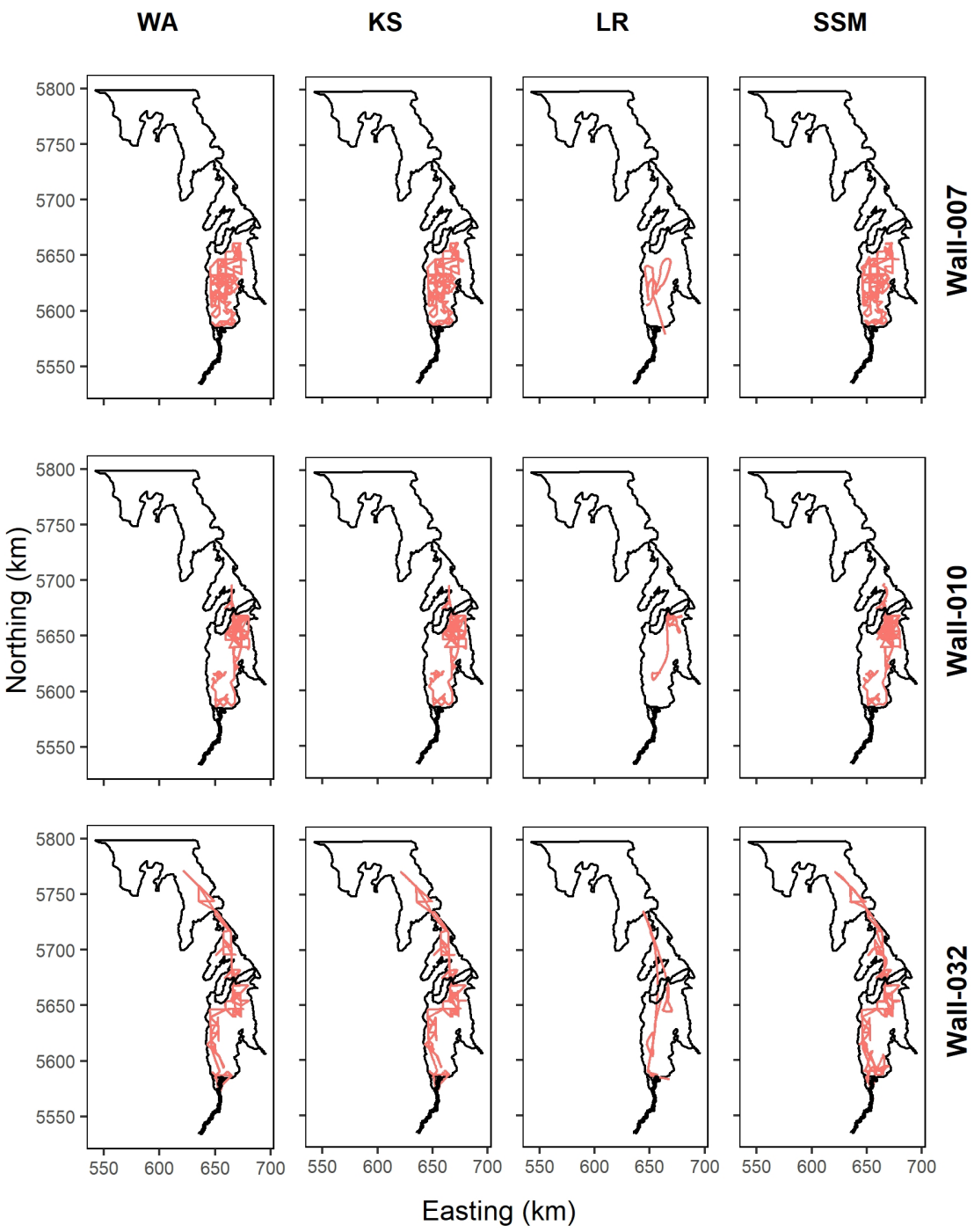

Figure 7: Reconstructed movement paths with the simple weighted average method (WA), kernel smoothing with the Gaussian kernel (KS), cross-validated local polynomial regression approach (LR), and the state-space modeling approach (SSM) for the fish "Wall-007", "Wall-010", and "Wall-032". Maps were made using R with ggplot2.

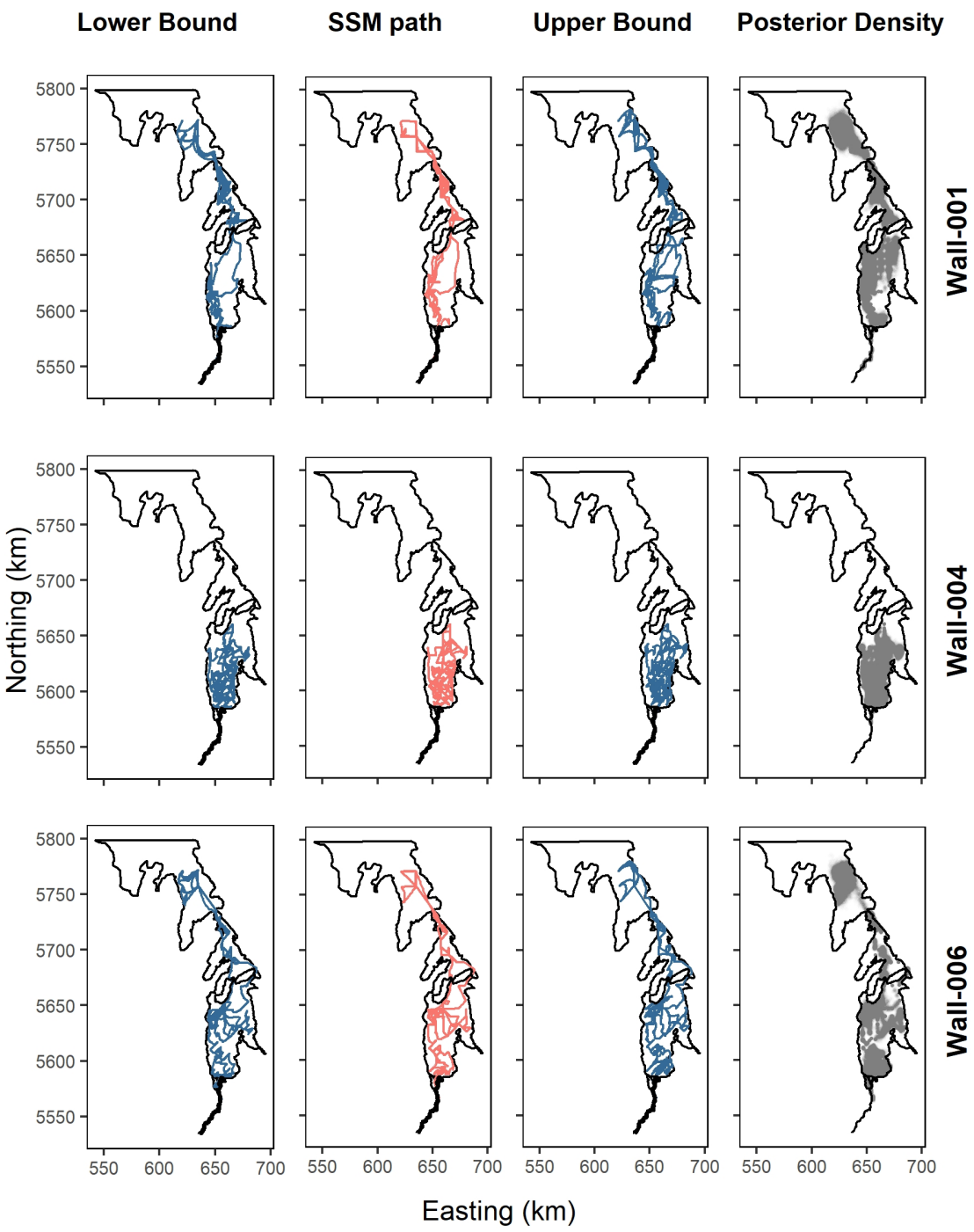

Figure 8: 95% credible paths and posterior density plots for the paths reconstructed with the SSM approach for the fish indexed "Wall-001", "Wall-004", and "Wall-006". Map made using R with ggplot2. Maps were made using R with ggplot2.

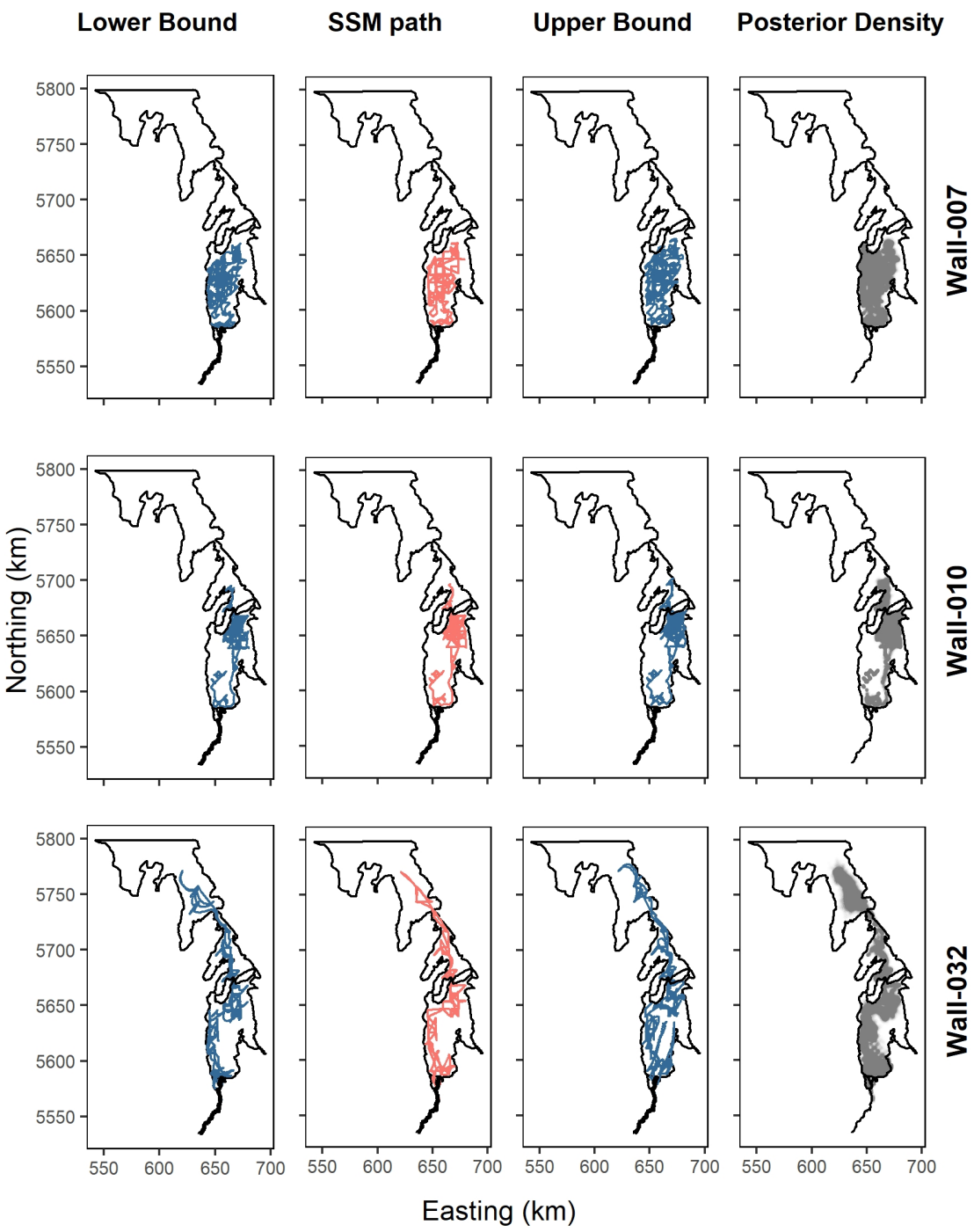

Figure 9: 95% credible paths and posterior density plots for the paths reconstructed with the SSM approach for the fish indexed "Wall-007", "Wall-010", and "Wall-032". Maps were made using R with ggplot2.